Astroclimate at San Pedro Mártir – I. Seeing statistics between 2004 and 2008 from the Thirty Meter Telescope site-testing data[★]

L. J. Sánchez,[1]† I. Cruz-González,[1] J. Echevarría,[1] A. Ruelas-Mayorga,[1] A. M. García,[1] R. Avila,[2] E. Carrasco,[3] A. Carramiñana[3] and A. Nigoche-Netro[4]

[1]*Instituto de Astronomía, Universidad Nacional Autónoma de México, Cd. Universitaria, México, D.F. 04510, México*
[2]*Centro de Física Aplicada y Tecnología Avanzada, Universidad Nacional Autónoma de México, Santiago de Querétaro, Qro. 76000, México*
[3]*Instituto Nacional de Astrofísica, Óptica y Electrónica, Tonantzintla, Pue. 72840, México*
[4]*Instituto de Astronomía y Meteorología, Universidad de Guadalajara, Guadalajara, Jal. 44130, México*

ABSTRACT

We present comprehensive seeing statistics for the San Pedro Mártir site derived from the Thirty Meter Telescope site-selection data. The observations were obtained between 2004 and 2008 with a Differential Image Motion Monitor (DIMM) and a Multi-Aperture Scintillation Sensor (MASS) combined instrument (MASS–DIMM). The parameters that are statistically analysed here are the whole atmosphere seeing (measured by the DIMM), the free atmosphere seeing (measured by the MASS) and the ground-layer (GL) seeing, which is the difference between the total seeing and the free atmosphere seeing. We have made a careful data coverage study, along with statistical distributions of simultaneous MASS–DIMM seeing measurements, in order to investigate the nightly, monthly, seasonal, annual and global behaviour, as well as possible hourly seeing trends. Although this campaign covers five years, the sampling is uneven, with 2006 and 2007 being the best sampled years in terms of seasonal coverage. The overall results yield a median seeing of 0.78 arcsec (DIMM), 0.37 arcsec (MASS) and 0.59 arcsec (GL). Therefore, the strongest contribution to the whole atmosphere seeing comes from a strong ground layer. We find that the best season is summer, while the worst season is winter, in accordance with previous studies. It is worth noting that the best yearly results are correlated with the best sampled years. The hourly analysis shows that there is no statistically significant tendency for seeing degradation towards dawn. The seeing values are slightly larger than those reported previously, which might be the result of climate changes.

Key words: atmospheric effects – site testing.

1 INTRODUCTION

In the early 1970s, a new observing site began operations at the Sierra de San Pedro Mártir (SPM), Baja California, Mexico. The site was selected using satellite photographs, and it was found to be one of the three best cloud-free areas in the world.

We now know that this site is one of the best astronomical locations in the world and it has been considered by the international astronomical community as a potential place for large telescopes to be built in the near future; it is a candidate site of projects such as the Large Synoptic Survey Telescope (LSST) and the Thirty Meter Telescope (TMT), as well as other astronomical projects.

Several climatological properties have been reported, mainly during the first years of operation of the Observatorio Astronómico Nacional (OAN) at SPM (Mendoza 1971, 1973; Mendoza et al. 1972; Alvarez & Maisterrena 1977; Alvarez & López 1982; Walker 1984) and later by Tapia (1992), Tapia (2003), Echevarría et al. (1998), Hiriart, Ochoa & García (2001), Michel, Hiriart & Chapela (2003c), Michel et al. (2003a), Carrasco & Sarazin (2003), Carrasco, Avila & Carramiñana (2005), Avila et al. (2006), Tapia, Cruz-González & Avila (2007a), Alvarez et al. (2007), Bohigas et al. (2008), Otárola et al. (2009), Bohigas & Núñez (2010), Araiza Quijano & Cruz-González (2011) and Carrasco et al. (2012).

Results on the seeing and optical turbulence above the ground can be found in Avila, Vernin & Cuevas (1998), Echevarría et al. (1998), Conan et al. (2002), Avila et al. (2007), Sánchez et al. (2007) and Avila et al. (2011), and results on atmosphere modelling

in Masciadri & Garfias (2001), Masciadri, Avila & Sánchez (2002, 2004), Masciadri et al. (2003) and Vogiatzis & Hiriart (2004). Extinction and opacity studies have also been performed by Schuster & Parrao (2001), Hiriart (2003) and Parrao & Schuster (2003). Site prospection studies within the SPM site have been carried out by Sohn (2007) and Bohigas et al. (2008). Comprehensive reviews on the site can be found in Cruz-González et al. (2003), Cruz-González et al. (2004), Tapia et al. (2007a), Tapia et al. (2007b) and Wehinger (2007).

In this paper, we analyse the data collected by the TMT Project Site Survey at the SPM site. We discuss and compare the results of the Differential Image Motion Monitor (DIMM) and a Multi-Aperture Scintillation Sensor (MASS) with previous studies. The observations include data in the time period 2004 October to 2008 February, analysed by Skidmore et al. (2009), plus data taken between 2008 February and 2008 August, the analysis of which has not been presented anywhere in the astronomical literature. Thus, we considerably improve the analysis of the complete TMT MASS–DIMM seeing survey at SPM and we supplement the seeing results published previously in the literature.

We also present, in a detailed manner, the number of observations and the percentage of time covered by them. This a novel way of treating seeing data.

With the aim of providing the astronomical community with detailed information of the seeing behaviour in SPM, we present nightly, monthly, seasonal, annual and global statistics. Also, we present an analysis of the hourly seeing trend, which yields different results from those found by Skidmore et al. (2009).

We give a summary of prior SPM seeing studies in Section 2. We present the SPM TMT site-testing instrumentation and data coverage in Section 3. We give the results and detailed statistics in Section 4.

2 SPM SITE: SEEING STUDIES

Atmospheric turbulence is usually studied by using a number of parameters, one of which is known as seeing (ε). The relation between ε, the Fried parameter r_o and the turbulence integral is given by

$$\varepsilon = 0.98 \frac{\lambda}{r_o} = 5.25 \lambda^{-1/5} \left[\int_0^\infty C_N^2(h)\,dh \right]^{3/5}, \qquad (1)$$

where λ is the wavelength and $\int_0^\infty C_N^2(h)\,dh$ is the optical turbulence energy profile (Roddier 1981).

We note that the seeing units are given in arcsec and, because seeing is a wavelength-dependent turbulence parameter, it is usually calculated for 0.5 µm. The seeing value is also corrected for the direction of observation and is referred to the zero zenith angle.

Early works on local SPM seeing conditions were carried out by Mendoza (1971) and Walker (1971). Several recent studies have been carried out by Echevarría et al. (1998), Conan et al. (2002) and Michel et al. (2003a). Optical turbulence studies have been performed by Avila et al. (1998), Avila et al. (2004), Avila et al. (2006), Avila et al. (2007) and Avila et al. (2011). A comprehensive review of some of these studies can be found in Echevarría (2003).

The observations of Echevarría et al. (1998) were obtained with two seeing monitors and a Micro Temperature Array tower (MTA); the Site-Testing Telescope (STT) from Steward Observatory was designed to observe Polaris, while the Carnegie Monitor (CM) could observe and track any star. The MTA consisted of platinum detectors, which measured temperature differences located at different heights, from 4 to 28 m. Echevarría et al. (1998) have reported a median seeing of 0.61 arcsec with a first quartile of 0.50 arcsec and a decrease of 0.1 arcsec at a height of 15 m. The STT observations covered 386 nights, while the CM observations covered 114 nights, spanning a three-year period. A summary of their results is shown in Table 1.

Conan et al. (2002) measured the wavefront outer scale and included ground-based seeing measurements with a DIMM. They reported observations during 31 nights. The telescope was located at two sites: at the CM tower and at a low-altitude location. They found a bimodal distribution during their 2000 December campaign with peaks centred at 0.50 and 0.75 arcsec, and an overall seeing median of 0.77 arcsec, including all observations during the 31-night period.

Michel et al. (2003a) conducted a study with the same DIMM during 123 nights spanning almost a three-year period. The monitor was located at the CM tower at a height of 8.3 m. They reported a median of 0.62 arcsec and a first quartile of 0.49 arcsec.

Skidmore et al. (2009) have analysed data collected by the TMT Project Site Survey at five different sites, which include SPM. A partial set (2004 October to 2008 February), of combined DIMM and MASS data, yields seeing median values of 0.58 arcsec for the ground layer, 0.37 arcsec for the free atmosphere and 0.79 arcsec for the whole atmosphere.

Concerning optical turbulence profiling, Avila et al. (1998, 2004) have monitored the vertical distribution of the optical turbulence strength using a Generalized SciDAR (GS). Two observation campaigns have been carried out at the OAN–SPM in 1997 and 2000. In 1997, the GS was installed at the 1.5-m and 2.1-m telescopes (SPM1.5 and SPM2.1) for eight and three nights (March and April), respectively, whereas in 2000 the instrument was

Table 1. SPM seeing monitoring results (whole atmosphere seeing).

Method	Reference	First quartile (arcsec)	Median (arcsec)	Third quartile (arcsec)	Nights
STT	Echevarría et al. (1998)	0.50	0.61		386
CM	Echevarría et al. (1998)	0.48	0.63		99
CM/STT[a]	Echevarría et al. (1998)	0.46	0.58		57
DIMM	Conan et al. (2002)		0.50; 0.75[b]		14
DIMM	Conan et al. (2002)	0.61	0.77	0.99	31
DIMM	Michel et al. (2003a)	0.48	0.60	0.81	123
MASS–DIMM	Skidmore et al. (2009)	0.61	0.79	1.12	[c]
SciDAR	Avila et al. (2011)	0.50	0.68	0.97	27

[a]CM simultaneous with STT.

[b]Bimodal distribution.

[c]From 2004 October to 2008 February.

installed for nine and seven nights (May) at SPM1.5 and SPM2.1, respectively.

Avila et al. (2011) performed a recalibration of the $C_N^2(h)$ profiles obtained at the OAN–SPM, following the results of a theoretical work on the normalization procedure used in the GS data reduction method (Avila & Cuevas 2009). From a statistical analysis of the recalibrated profiles, Avila et al. (2011) have found that the seeing in the first two kilometres, in the free atmosphere and in the whole atmosphere had median values of 0.38, 0.35 and 0.68 arcsec, respectively.

Table 1 shows a synthesis of the non-differential monitors (STT and CM), differential (DIMM) and SciDAR seeing monitoring campaigns.

3 TMT SITE-TESTING DATA

3.1 The 2004–2008 TMT site-testing campaign

SPM was one of the five candidate sites selected by the TMT site-testing team (Schöck et al. 2009). Three Southern hemisphere sites were studied – Cerros Tolar, Armazones and Tolonchar in northern Chile – and two Northern hemisphere sites – the 13 North (13 N) site on Mauna Kea, Hawaii in the United States and SPM in Mexico. During a period of approximately five years, from 2004 to 2008, the TMT group measured the atmospheric properties of each site with the same instrumentation, and at least 2.5 annual cycles of data were acquired at each of the candidate sites. As described in detail by Schöck et al. (2009), a suite of eight instruments were deployed at the candidate sites. The data acquisition methodology has also been presented in their work. The acquired data of all the instruments have kindly been made available to the public at http://sitedata.tmt.org/ by the TMT organization.

3.2 Seeing instrumentation

The SPM TMT T4 site-testing station was equipped with a 35-cm telescope mounted approximately 7 m above ground. At the Cassegrain focus of the telescope, a combined instrument was deployed, which included a DIMM and a MASS, hereafter called MASS–DIMM, described by Kornilov et al. (2007). Combined MASS–DIMM instruments are extensively used for seeing measurements and optical turbulence profiling (e.g. Tokovinin et al. 2003, 2005).

The DIMM channel measures the wavefront slope differences over two small pupils some distance apart. This yields the whole atmosphere seeing from the telescope level to the top of the atmosphere (Sarazin & Roddier 1990). DIMM seeing measurements ε_{DIMM} are affected by different sources of bias, such as image threshold, defocus, exposure time, photon noise and high-frequency vibrations that must be monitored in real time; thus, some of the measurements are rejected. In particular, for the system used here, the precision reported is better than 0.02 arcsec (Wang et al. 2007).

The MASS channel detects rapid variations of light intensity in four concentric apertures using photomultipliers, and it reconstructs a turbulence profile at six different heights above the telescope (Tokovinin & Kornilov 2007). The MASS is not sensitive to turbulence near the ground because this does not produce any scintillation and it can only measure the seeing in the free atmosphere (FA), thus excluding the ground layer. So, we have $\varepsilon_{MASS} = \varepsilon_{FA}$. From the turbulence profile, the seeing integrated from 500 m above the telescope to the top of the atmosphere is computed. The MASS seeing accuracy is better than 0.05 arcsec (Els et al. 2008).

3.3 SPM TMT data coverage

The SPM TMT T4 station acquired MASS–DIMM data from 2004 October to 2008 August. The DIMM and MASS nightly operations commenced one hour after sunset and ceased one hour before sunrise. The DIMM and MASS measurements were triggered simultaneously. The DIMM took integrated stellar light measurements during a time interval of 36 s, whereas the MASS sampled light during 60-s periods. Because the DIMM channel was used to acquire the target star, this resulted in simultaneous MASS–DIMM measurements every 70–90 s (Els et al. 2009). Sometimes, computations failed to provide valid results, probably because of cloudy conditions or technical problems, while sometimes the telescope system was shutdown as a result of bad weather conditions.

In Fig. 1, we present the total amount of DIMM, MASS and simultaneous MASS–DIMM data for each month during the acquisition period. By simultaneous MASS–DIMM data, we mean measurements within the same minute interval.

We have also computed the statistics of the data coverage per night and per month. In order to compute the monthly temporal data coverage, we have considered the duration for each night of the year as a result of the diurnal cycle variation. This yields a percentage value of the available data for each night in a given month. A 100 per cent value would indicate data obtained during the whole night for every night of the month.

To the best of our knowledge, this is the first time that a complete data coverage of seeing observations has been presented in the astronomical literature. Whereas, in other papers, the number of nights observed is spoken of, regardless of whether one seeing point or many have been observed per night, we emphasize the effective length of time observed per night, making this a novel way of treating seeing data.

Tables 2, 3 and 4 give the percentage of monthly, seasonal and annual data coverage of DIMM, MASS and simultaneous MASS–DIMM, respectively, during the acquisition period.

In Figs 2, 3 and 4, we present grey-level plots showing only the monthly percentage of data coverage for the 2004–2008 period for DIMM, MASS and simultaneous MASS–DIMM, respectively, extracted from Tables 2, 3 and 4.

These figures are intended to be a visual aid in order to see, at a glance, which months are those with the best coverage. The degree of darkening corresponds to the monthly percentage values presented in Tables 2, 3 and 4.
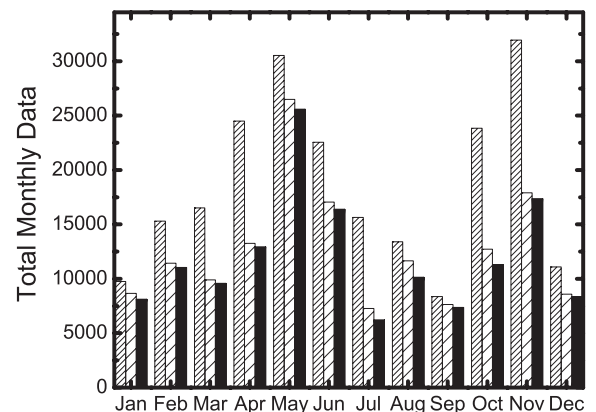

Figure 1. Total monthly data for the 2004–2008 period: DIMM (dense shading), MASS (sparse shading) and simultaneous MASS–DIMM (dark).

Table 2. Amount of data collected and coverage percentage for DIMM.

Month	2004		2005		2006		2007		2008		Total	
						Year						
January	–	–	129	0.9%	3371	23.1%	6263	43.1%	0	0.0%	9763	16.8%
February	–	–	0	0.0%	3082	23.5%	7767	60.9%	4449	35.5%	15 298	30.0%
March	–	–	0	0.0%	5740	46.3%	5992	47.0%	4794	38.9%	16 526	33.0%
Winter											41 587	26.6%
April	–	–	2846	25.5%	8185	74.4%	3901	36.4%	9557	86.7%	24 489	55.7%
May	–	–	6755	64.9%	7640	73.5%	8472	81.5%	7657	73.6%	30 524	73.4%
June	–	–	5740	59.9%	6609	69.0%	3959	41.4%	6233	65.1%	22 541	58.8%
Spring											77 554	62.6%
July	–	–	628	6.3%	5064	50.3%	5792	57.7%	4155	41.2%	15 639	38.9%
August	–	–	0	0.0%	6578	60.3%	6174	56.1%	642	6.1%	13 394	30.6%
September	–	–	0	0.0%	8361	71.2%	0	0.0%	–	–	8361	23.8%
Summer											37 394	31.1%
October	6081	45.5%	445	3.2%	8712	66.1%	8612	63.7%	–	–	23 850	44.6%
November	3887	28.0%	10 134	73.6%	9916	72.1%	8004	57.7%	–	–	31 941	57.8%
December	0	0.0%	5165	35.1%	5933	40.3%	0	0.0%	–	–	11 098	18.8%
Autumn											66 889	40.4%
Total	9968	36.7%	31 842	22.4%	79 191	55.8%	64 936	45.4%	37 487	43.4%	223 424	40.2%

Table 3. Amount of data collected and coverage percentage for MASS.

| Month	2004		2005		2006		2007		2008		Total	
						Year						
January	–	–	241	1.7%	2663	18.2%	5768	39.7%	0	0.0%	8672	14.9%
February	–	–	0	0.0%	2448	18.7%	6451	50.6%	2536	20.3%	11 435	22.4%
March	–	–	0	0.0%	4669	37.7%	4890	38.4%	354	2.7%	9913	19.7%
Winter											30 020	19.0%
April	–	–	2414	21.6%	7283	66.3%	3562	33.2%	0	0.0%	13 259	30.3%
May	–	–	6164	59.1%	6846	65.9%	7366	70.9%	6106	58.7%	26 482	63.6%
June	–	–	5006	52.3%	5516	57.5%	3266	34.2%	3274	34.2%	17 062	44.5%
Spring											56 803	46.1%
July	–	–	463	4.6%	4509	44.8%	2294	22.8%	0	0.0%	7266	18.1%
August	–	–	0	0.0%	5816	53.3%	5837	53.6%	0	0.0%	11 653	26.7%
September	–	–	0	0.0%	7641	65.2%	0	0.0%	–	–	7641	21.7%
Summer											26 560	22.2%
October	5159	38.9%	336	2.5%	7223	54.7%	0	0.0%	–	–	12 718	24.0%
November	3436	25.5%	7428	53.7%	6786	49.3%	263	1.9%	–	–	17 913	32.6%
December	0	0.0%	3908	26.6%	4687	31.8%	0	0.0%	–	–	8595	14.6%
Autumn											39 226	23.7%
Total	8595	21.5%	25 960	18.5%	66 087	46.9%	39 697	28.8%	12 270	14.5%	152 609	27.9%

At first glance, we immediately notice two main features: (i) the best coverage was obtained during 2006 and 2007; (ii) April, May and June are the best covered months.

This is further supported by a careful analysis of Tables 2, 3 and 4. For 2006 and 2007, the DIMM data coverage is 55.8 and 45.4 per cent, respectively, while the MASS coverage for these years is 46.9 and 28.8 per cent, respectively. The simultaneous MASS–DIMM coverage is 45.3 and 26.4 per cent, respectively. The overall data coverage for all years is significantly less (DIMM, 40.2 per cent; MASS, 27.9 per cent; simultaneous MASS–DIMM, 26.4 per cent). Although these coverage values are low, they reflect the enormous difficulties in obtaining seeing data, even in experiments designed

Table 4. Amount of data collected and coverage percentage for simultaneous MASS–DIMM.

Month	2004		2005		2006		2007		2008		Total	
January	–	–	63	0.4%	2613	17.9%	5451	37.5%	0	0.0%	8127	14.0%
February	–	–	0	0.0%	2394	18.2%	6152	48.3%	2490	20.0%	11036	21.6%
March	–	–	0	0.0%	4521	36.5%	4713	37.0%	352	2.7%	9586	19.1%
Winter											28749	18.2%
April	–	–	2399	21.5%	7129	64.9%	3422	31.9%	0	0.0%	12950	29.6%
May	–	–	5779	55.4%	6707	64.5%	7156	68.9%	5946	57.2%	25588	61.5%
June	–	–	4857	50.7%	5331	55.6%	3088	32.3%	3117	32.5%	16393	42.8%
Spring											54931	44.6%
July	–	–	340	3.4%	4134	41.0%	1751	17.6%	0	0.0%	6225	15.5%
August	–	–	0	0.0%	5625	51.5%	4511	41.1%	0	0.0%	10136	23.2%
September	–	–	0	0.0%	7360	62.8%	0	0.0%	–	–	7360	20.9%
Summer											23721	19.9%
October	4033	30.5%	337	2.5%	6941	52.6%	0	0.0%	–	–	11311	21.4%
November	3259	24.2%	7274	52.6%	6607	48.0%	241	1.7%	–	–	17381	31.6%
December	0	0.0%	3819	25.9%	4451	30.2%	0	0.0%	–	–	8270	14.0%
Autumn											36962	22.3%
Total	7292	18.2%	24868	17.7%	63813	45.3%	36485	26.4%	11905	14.1%	144363	26.4%
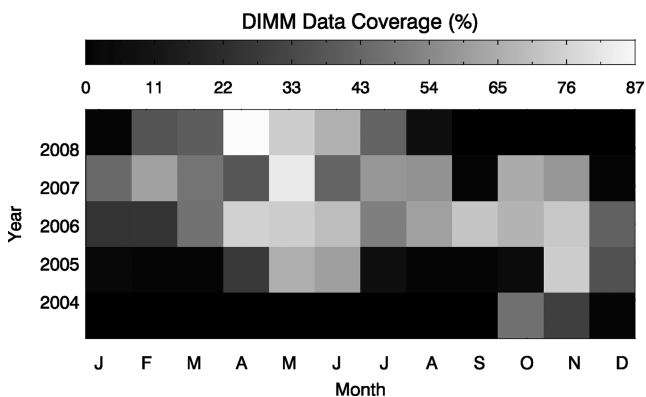
Figure 2. Grey-level plot showing the monthly percentage of data coverage for the 2004–2008 period for DIMM. A black square means that no usable data were available.
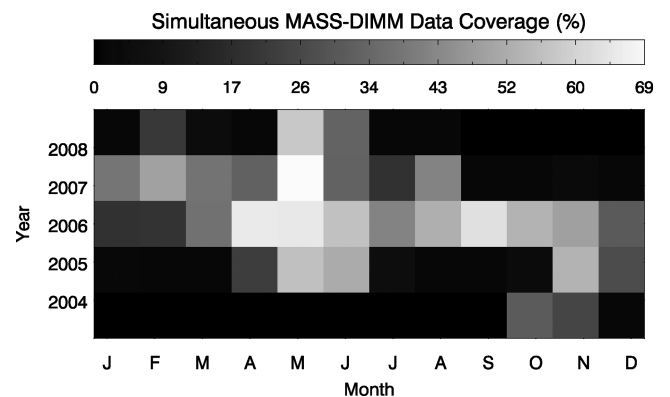
Figure 4. Grey-level plot showing the monthly percentage of data coverage for the 2004–2008 period for simultaneous MASS–DIMM. A black square means that no usable data were available.
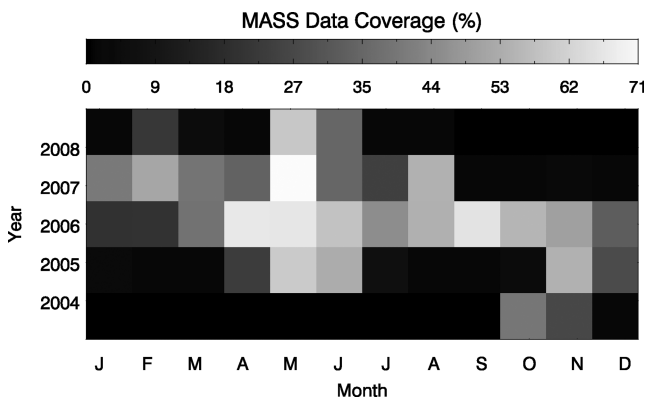
Figure 3. Grey-level plot showing the monthly percentage of data coverage for the 2004–2008 period for MASS. A black square means that no usable data were available.

to ensure high data collection efficiencies, as is the case for the TMT site-testing data (Riddle, Schöck & Skidmore 2006; Schöck et al. 2010). Note that the best sampled year for simultaneous measurements is 2006 (45.3 per cent) and the worst sampled year is 2008 (14.1 per cent).

Seasonal MASS–DIMM coverage in winter is 18.2 per cent, in spring it is 44.6 per cent, in summer it is 19.9 per cent and in autumn it is 22.3 per cent. Seasons have been defined at the beginning of the month: winter (January, February and March), spring (April, May and June), summer (July, August and September) and autumn (October, November and December).

In the monthly case, we can see that the data coverage is worse in January (14.0 per cent), December (14.0 per cent) and July (15.5 per cent), while the best sampled months are May (61.5 per cent), June (42.8 per cent) and November (31.6 per cent).
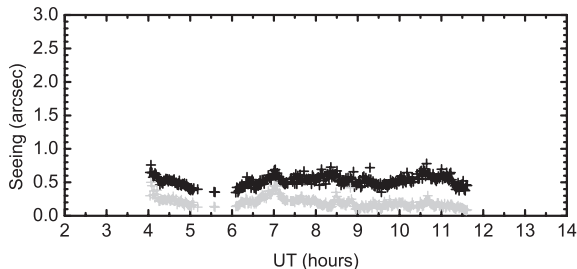
Figure 5. Example of DIMM (upper curve) and MASS (lower curve) seeing median values during a good steady night (2007-08-12).
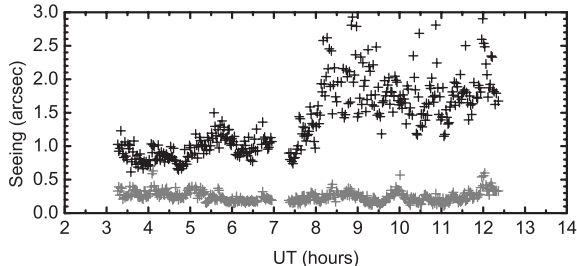

Figure 6. Example of DIMM (upper curve) and MASS (lower curve) seeing median values during a night on which only DIMM seeing degrades during the night (2006-03-21).

4 RESULTS

We have calculated the seeing from MASS, DIMM and simultaneous MASS–DIMM, obtaining nightly, monthly, seasonal, annual and global statistics (first quartile, median and third quartile, via cumulative distributions). The behaviour of the measured seeing expressed as $\log(\varepsilon)$ was verified to follow normal statistics. We obtained an expected correlation between seeing coverage percentage and deviations from a lognormal distribution. The seeing distribution is expected to be lognormal because ε is a random variable that ranges from 0 to infinity. Fried & Mevers (1974) confirmed r_o as a lognormally distributed random variable.

4.1 Nightly statistics

We have made a nightly analysis of all available data ($\sim$800 nights of DIMM data, $\sim$620 nights of MASS data and $\sim$600 nights of simultaneous data, out of $\sim$1400 nights, which corresponds to the total length of the campaign), which are either partially covered or fully covered nights. We found a great variety for the behaviour of both the DIMM and the MASS: nights with excellent seeing throughout the night; erratic seeing nights; degrading seeing, in which there is a sudden burst of bad seeing, etc. In the following paragraphs, we discuss a couple of examples.

In Fig. 5, we present one night (2007 August 12) with good steady seeing. For both DIMM and MASS, the seeing variations are well correlated. The median seeing measured by DIMM and MASS is 0.53 and 0.19 arcsec, respectively.

In Fig. 6, we present one night (2006 March 21) in which it is clear that there is a strong lack of correlation between the DIMM and MASS seeing. Only the DIMM seeing degraded during the night, while the MASS seeing remained steady with a median of 0.24 arcsec.

The median standard variation of the whole atmosphere seeing within a night is 0.19 arcsec (with first and third quartiles 0.12 and 0.29 arcsec, respectively).

As an example of simultaneous MASS–DIMM nightly statistics, we show in the left panels of Figs 7 and 8, the seeing median values for some of the best sampled months (2006 September with 25 nights and 2007 August with 24 nights).

4.2 Monthly statistics

In Table 5, we present detailed monthly statistics for DIMM and MASS data for the whole campaign.

Apart from the worst median seeing value obtained in 2005 January, which happens to be the month with the poorest coverage (0.4 per cent; see Table 4), DIMM seeing values vary from 0.6 to 1.1 arcsec and MASS seeing values vary from 0.3 to 0.4 arcsec. An example of monthly statistics is shown in the right panels of Figs 7 and 8, which contain the seeing cumulative distribution functions (CDFs) for the same months previously mentioned. For DIMM, we obtain a median seeing of 0.62 and 0.61 arcsec, respectively, while for MASS we obtain 0.31 and 0.27 arcsec, respectively.

4.3 Seasonal statistics

In Fig. 9, we show the seeing seasonal behaviour. For each season, we plot the DIMM and MASS median seeing values for the corresponding months. The DIMM seeing displays a pronounced seasonal variability, and there seems to be a slight correlation between the DIMM and MASS variations. It is clear that the worst whole atmosphere seeing occurs in winter, although at the end of the season there is a tendency towards a better seeing. This tendency continues until the middle part of summer, when the best seeing is achieved, worsening progressively towards autumn.

In the upper part of Table 6, we present the seasonal statistics for the entire observing run. As mentioned above, the worst whole atmosphere seeing occurs in winter (0.97 arcsec) and the best in summer (0.64 arcsec).

The differences in seasonal MASS are smaller, indicating that most of the large DIMM seeing variations are a result of turbulence occurring near the ground (see Section 4.5).

4.4 Annual statistics

In Figs 10 and 11, we present the DIMM and MASS seeing measurements for the years 2006 and 2007, which are the best sampled years in terms of seasonal coverage.

In both figures, we can see a clear seasonal variation of the DIMM seeing, whereas the MASS values tend to remain more stable throughout the year.

The lower part of Table 6 presents the yearly DIMM and MASS statistics. It is interesting to note that the best whole atmosphere seeing occurs for 2006 (0.74 arcsec), which is the best sampled year.

4.5 Ground-layer statistics

We calculated the ground-layer (GL) seeing ε_{GL} (from 7 to 500 m), which is defined as the difference between the DIMM and MASS seeing. As we note from equation (1), the contributions of the different layers to the seeing must be summed as the 5/3 power, which yields

$$\varepsilon_{GL} = \left(\varepsilon_{DIMM}^{5/3} - \varepsilon_{MASS}^{5/3} \right)^{3/5}. \tag{2}$$

In the data acquisition process, it might occur that $\varepsilon_{DIMM} < \varepsilon_{MASS}$. These occurrences correspond to what Tokovinin (2007)
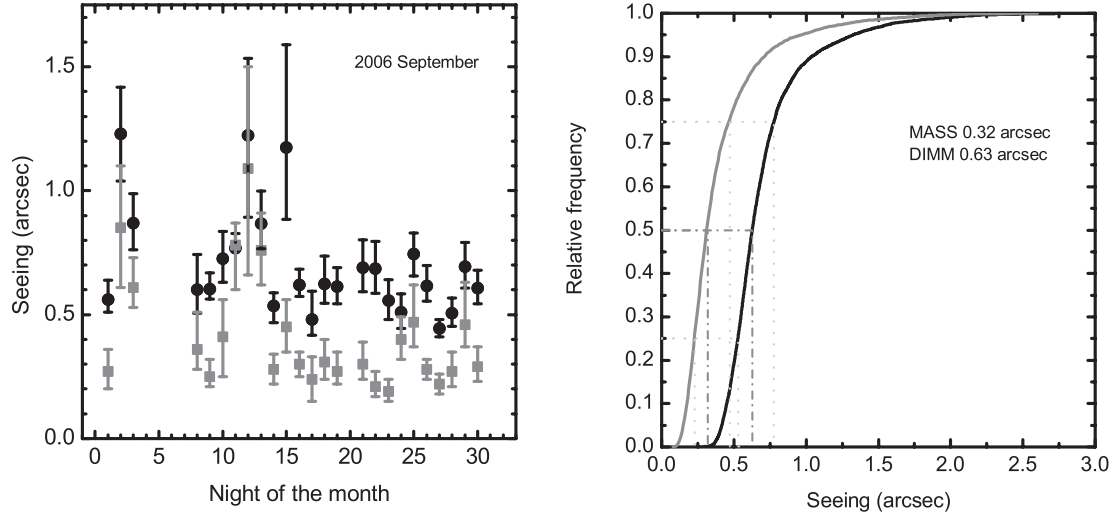
Figure 7. Left panel: DIMM (circles) and MASS (squares) statistics for simultaneously obtained data. Median seeing values (with lower and upper limits represented by first and third quartiles, respectively) for each night of the month in 2006 September. Right panel: seeing CDF for the same month. The left curve represents MASS values with a median of 0.32 arcsec, and the right curve represents DIMM values with a median of 0.63 arcsec.
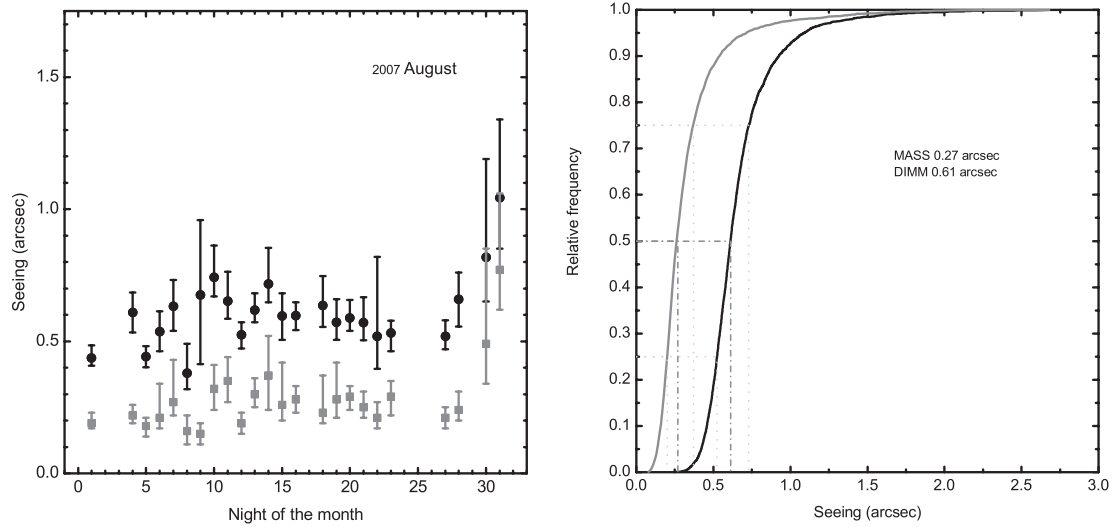

Figure 8. Left panel: DIMM (circles) and MASS (squares) statistics for simultaneously obtained data. Median seeing values (with lower and upper limits represented by first and third quartiles, respectively) for each night of the month 2007 August. Right panel: seeing CDF for the same month. The left curve represents MASS values with a median of 0.27 arcsec, and the right curve represents DIMM values with a median of 0.61 arcsec.

Table 5. Median seeing monthly values (arcsec).

| Month	2004		2005		2006		2007		2008		Total	
	DIMM	MASS	DIMM	MASS	DIMM	MASS	DIMM	MASS	DIMM	MASS	DIMM	MASS
January	–	–	1.47	0.82	0.75	0.36	1.10	0.47	–	–	1.01	0.44
February	–	–	–	–	1.07	0.52	0.98	0.41	0.86	0.34	0.99	0.41
March	–	–	–	–	1.08	0.33	0.82	0.39	0.96	0.50	0.92	0.37
April	–	–	0.98	0.40	0.83	0.37	0.92	0.45	–	–	0.88	0.40
May	–	–	0.77	0.28	0.64	0.30	0.76	0.30	0.89	0.43	0.75	0.32
June	–	–	0.84	0.30	0.74	0.41	0.73	0.39	0.65	0.33	0.75	0.36
July	–	–	0.94	0.59	0.72	0.46	0.58	0.30	–	–	0.68	0.41
August	–	–	–	–	0.64	0.35	0.61	0.27	–	–	0.63	0.31
September	–	–	–	–	0.62	0.31	–	–	–	–	0.62	0.31
October	1.08	0.46	0.85	0.33	0.75	0.38	–	–	–	–	0.83	0.40
November	0.97	0.41	0.83	0.42	0.83	0.40	0.89	0.52	–	–	0.85	0.41
December	–	–	0.78	0.38	0.82	0.38	–	–	–	–	0.80	0.38
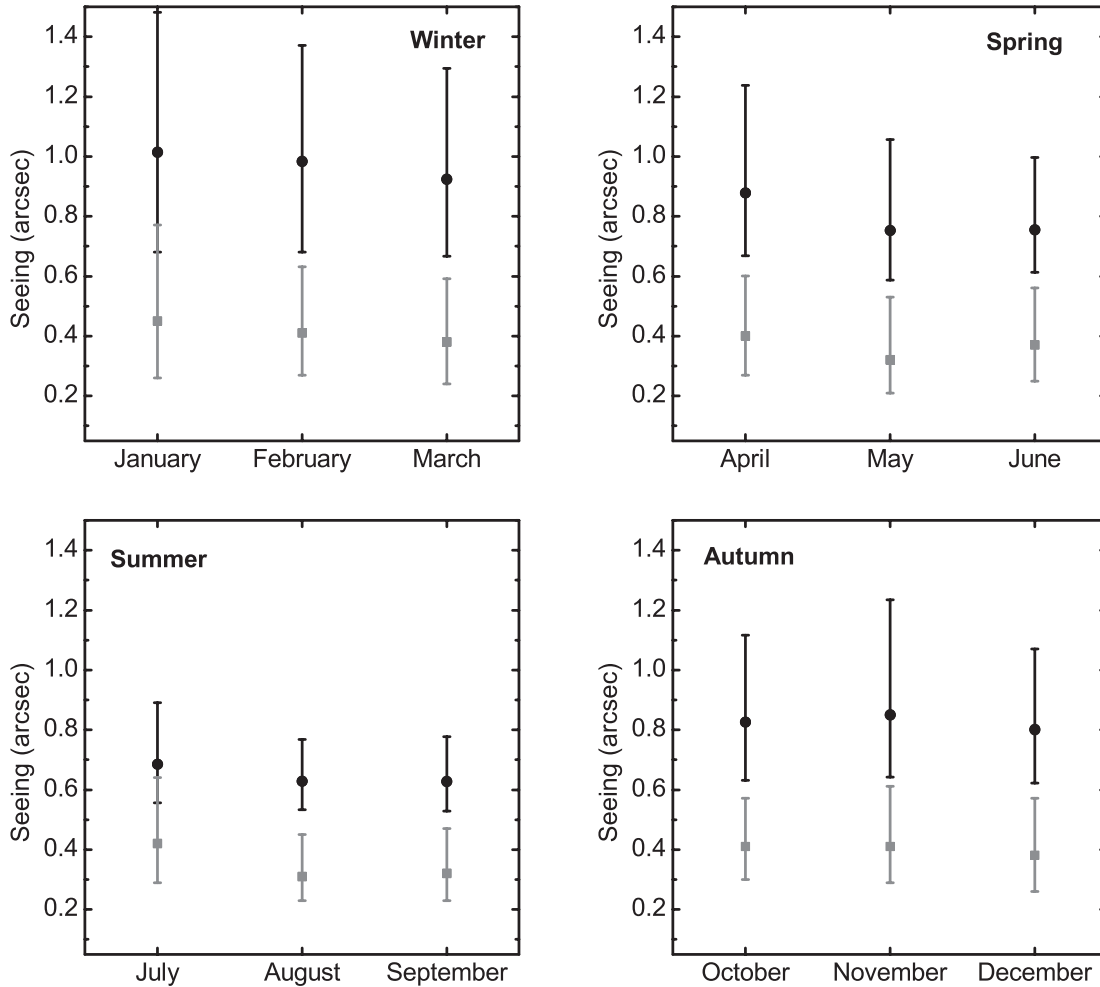
Figure 9. Median seeing values (with first and third quartiles as error bars) for each month of every season covered by the campaign (2004–2008). Symbols as in Fig. 7, left panel.

Table 6. Seasonal and annual seeing statistics (arcsec).

Season	DIMM First quartile	Median	Third quartile	MASS First quartile	Median	Third quartile	Ground layer First quartile	Median	Third quartile	Coverage per cent
Winter	0.67	0.97	1.38	0.26	0.40	0.64	0.51	0.73	1.11	18.2
Spring	0.61	0.78	1.07	0.23	0.35	0.54	0.46	0.59	0.81	44.6
Summer	0.54	0.64	0.79	0.24	0.33	0.48	0.38	0.46	0.56	19.9
Autumn	0.64	0.83	1.16	0.28	0.40	0.58	0.46	0.63	0.92	22.3
Year										
2004	0.72	1.04	1.51	0.31	0.44	0.65	0.56	0.81	1.27	18.2
2005	0.65	0.82	1.13	0.24	0.36	0.54	0.49	0.65	0.89	17.7
2006	0.58	0.74	1.02	0.25	0.37	0.55	0.42	0.54	0.76	45.3
2007	0.60	0.80	1.17	0.24	0.37	0.58	0.46	0.60	0.87	26.4
2008	0.61	0.82	1.11	0.26	0.38	0.57	0.45	0.62	0.86	14.1

defined as 'over-shoots'. We have found that the total number of these occurrences corresponds to ~1.5 per cent. We have decided to reject these data; we note that the amount of rejected data is small, and therefore the overall statistics of the GL seeing are not affected.

In the GL section of Table 6, we present the seasonal and yearly results for the GL seeing values. In Table 7, we show the monthly variation of the GL seeing for the entire observing run. We note that the best GL seeing is during July, August and September months, with a value ~0.46 arcsec.

Again, the GL behaviour is similar to the DIMM seeing; it is best in summer and worst in winter. This is because the MASS values are always nearly constant, showing that the high-altitude turbulence at SPM is small. Therefore, the main contribution to the whole atmosphere seeing at SPM comes from a strong GL.
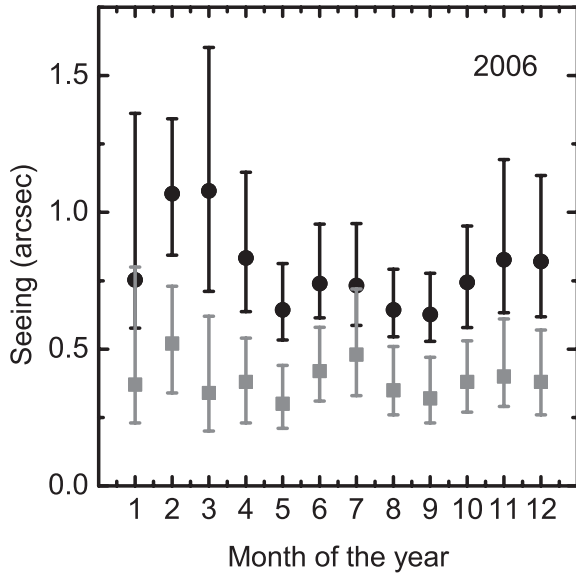
Figure 10. DIMM (circles) and MASS (squares) simultaneously obtained data. Median seeing values (with first and third quartiles as error bars) for each month of 2006.
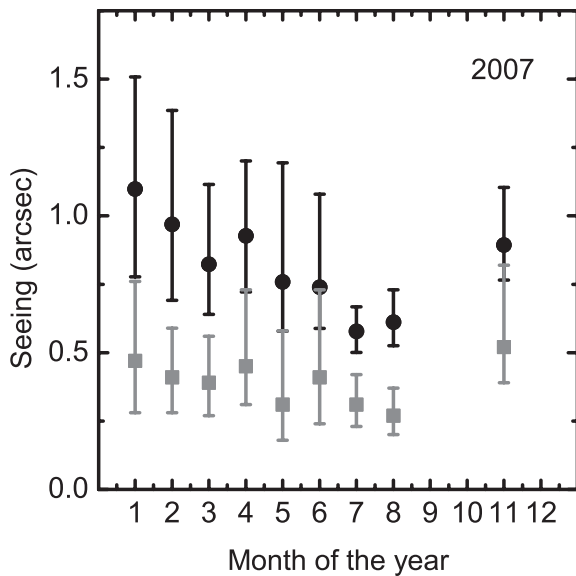

Figure 11. DIMM (circles) and MASS (squares) simultaneously obtained data. Median seeing values (with first and third quartiles as error bars) for each month of 2007.

4.6 Global statistics and hourly trend

In the left panel of Fig. 12 we show the CDF for the DIMM, MASS and derived GL seeing for all simultaneous data. Table 8 shows the overall seeing results.

Skidmore et al. (2009) have argued that the DIMM seeing at SPM rises during the second half of the night (see their fig. 4). We decided to explore the seeing behaviour and to look for a possible degradation during the night. In Fig. 13, we have plotted the number of data as a function of the hour at which they were taken. It is clear that before 4 UT hours and after 11 UT hours, the number of measurements taken was substantially smaller than within 4–11 UT. This justifies the calculation of an overall CDF in this restricted

Table 7. Ground-layer monthly median seeing (arcsec).

Month	2004	2005	2006	2007	2008	Total
January	–	0.97	0.60	0.82	–	0.76
February	–	–	0.77	0.76	0.72	0.75
March	–	–	0.89	0.61	0.67	0.69
April	–	0.78	0.64	0.65	–	0.66
May	–	0.65	0.50	0.58	0.65	0.58
June	–	0.68	0.53	0.53	0.49	0.57
July	–	0.64	0.45	0.42	–	0.45
August	–	–	0.46	0.48	–	0.47
September	–	–	0.47	–	–	0.47
October	0.81	0.72	0.56	–	–	0.63
November	0.80	0.61	0.62	0.61	–	0.64
December	–	0.58	0.62	–	–	0.60

range, presented in the right panel of Fig. 12. The second line of Table 8 shows the overall results only for the same interval. As is clear, the resulting statistics does not significantly change when using the restricted time interval.

In Fig. 14, we plot the DIMM and MASS hourly results integrated over the whole campaign. The seeing seems to be worse at the beginning and at the end of the night. However, the number of data (N) that support this assertion is small, and it is clear from the figure that these data correspond to the longest nights of the year (i.e. winter nights where seeing is usually worse). The points on the plot have error bars corresponding to $1/\sqrt{N}$.

We have made a weighted fifth grade polynomial fit to the points. It is clear that in the interval delimited by the vertical dotted lines (corresponding to the shortest night of the year), the fit is essentially linear and horizontal, which might indicate that the seeing remains constant throughout the night. We know that by giving the data points an error bar equal to $1/\sqrt{N}$, those points within the 4–11 UT interval (where N is sufficiently large) have a determinant influence on the results of the fit. However, it is correct to do it this way, because we have shown that the statistical results in the 4–11 UT interval are the same as those for the whole interval (see Table 8).

In order to explore, with precision, the seeing behaviour at the beginning and the end of the night, we analyse the data in a different manner – we integrate with respect to the astronomical dusk and to the astronomical dawn, calculated for each night of the year. We do this because the beginning and the end of the night occur at a different time (UT) throughout the year.

We include Figs 15 and 16, which show the median seeing versus hours after astronomical dusk and before astronomical dawn, respectively.

Performing a linear fit to the DIMM points contained within the length of the shortest night, we find it to be essentially flat with slopes $9.0311 \times 10^{-4} \pm 0.0016$ for Fig. 15 and 0.0024 ± 0.0016 for Fig. 16.

The MASS points do not seem to show any significant tendency in either case, with slopes of $3.9400 \times 10^{-4} \pm 0.0016$ and $-2.4118 \times 10^{-4} \pm 0.0016$.

Thus, we conclude that the seeing at SPM does not statistically change either shortly after dusk or towards the last few hours of the night, in contrast with the results reported by Skidmore et al. (2009), and in good agreement with the findings of Echevarría et al. (1998) and Sánchez et al. (2003) where no clear tendency was found.
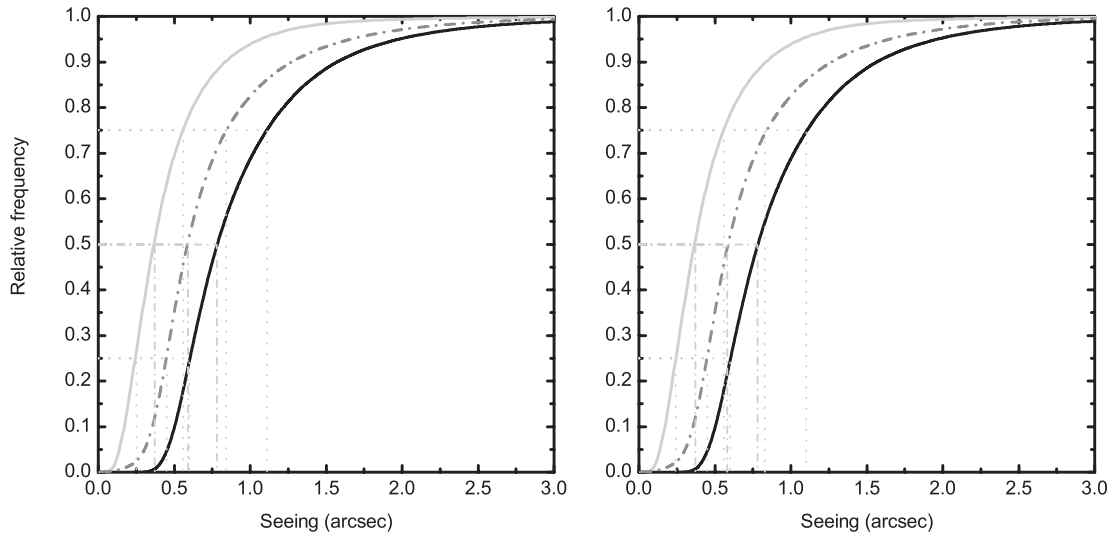
Figure 12. MASS, DIMM and GL statistics for simultaneously obtained data. Left panel: CDFs for the whole campaign (2004–2008) including all data points: median(MASS) = 0.37 arcsec; median(DIMM) = 0.78 arcsec; median(GL) = 0.59 arcsec. Right panel: CDFs for the whole campaign (2004–2008) including only 4–11 UT data points: median(MASS) = 0.37 arcsec; median(DIMM) = 0.77 arcsec; median(GL) = 0.58 arcsec. Left curves represent MASS values, middle curves represent GL values and right curves represent DIMM values.

Table 8. Global seeing statistics (arcsec).

Data	DIMM			MASS			Ground layer		
	First quartile	Median	Third quartile	First quartile	Median	Third quartile	First quartile	Median	Third quartile
All	0.60	0.78	1.11	0.25	0.37	0.56	0.45	0.59	0.84
4–11 UT	0.60	0.78	1.10	0.24	0.37	0.56	0.45	0.58	0.83
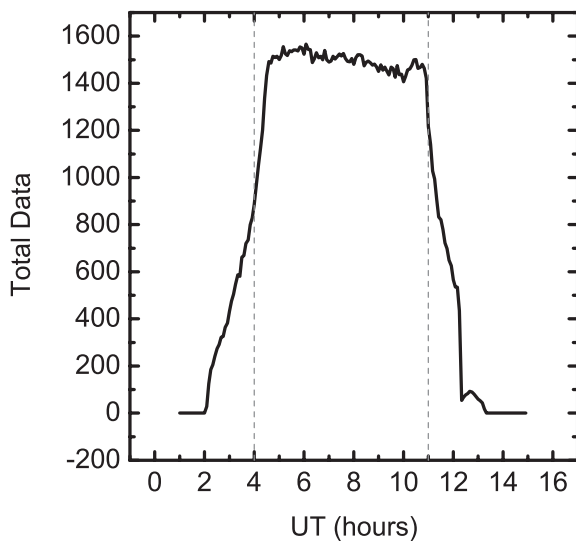
Figure 13. Total number of hourly simultaneous DIMM and MASS measurements (N). The vertical lines delimit the interval between 4 and 11 UT hours.

Figure 14. Hourly seeing computed from total simultaneous DIMM (upper curve) and MASS (lower curve) data. The error bars correspond to $1/\sqrt{N}$. The fitted curve to the DIMM data corresponds to a weighted fifth degree polynomial. Vertical dotted lines indicate the shortest night, whereas vertical dash-dotted lines delimit the longest night of the year.

4.7 Comparison with previous results

Our seasonal results (see Section 4.3) can be compared with the findings of Echevarría et al. (1998) with the STT and CM monitors and those of Michel et al. (2003b) with a DIMM monitor. Echevarría et al. (1998) found a summer median of 0.58 arcsec while Michel et al. (2003b) found a median of 0.55 arcsec, compared with the
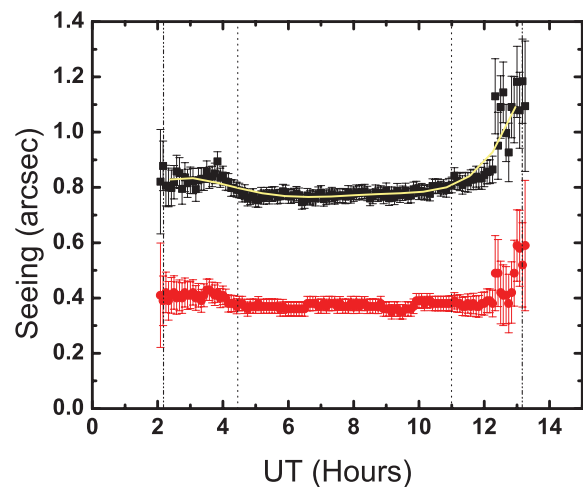
value of 0.64 arcsec obtained here. Although we find higher values in all seasons in this paper, summer is still shown to be the best season in all studies. We point out that the coverage percentages in summer, autumn and winter, presented in this paper, are particularly low (≤23 per cent). Still, the median value for spring is much higher than in previous works: 0.60 arcsec in Echevarría et al. (1998), 0.61
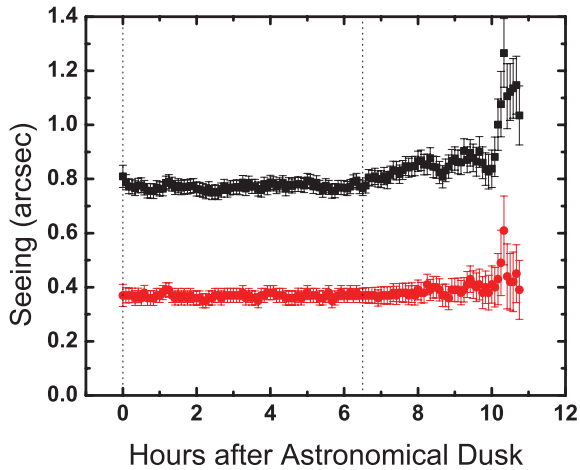
Figure 15. Hourly seeing computed from total simultaneous DIMM (upper curve) and MASS (lower curve) data, for hours after astronomical dusk. The error bars correspond to $1/\sqrt{N}$. Vertical dotted lines delimit the shortest night of the year.
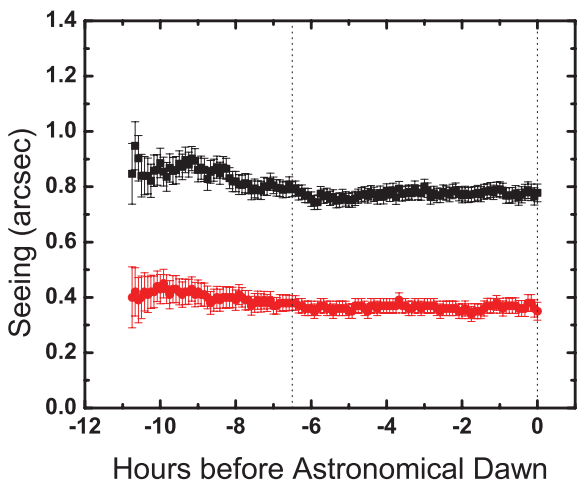

Figure 16. Hourly seeing computed from total simultaneous DIMM (upper curve) and MASS (lower curve) data, for hours before astronomical dawn. The error bars correspond to $1/\sqrt{N}$. Vertical dotted lines delimit the shortest night of the year.

arcsec in Michel et al. (2003b) and 0.78 in this paper. The results for autumn are 0.68, 0.63 and 0.83 arcsec respectively, while the results for winter are 0.69, 0.77 and 0.97 arcsec, respectively. Thus, the results are consistent, if not in absolute values, in the fact that summer yields the best values, while winter is the worst season. The mean values for all three campaigns are 0.79, 0.68, 0.61 and 0.70 arcsec for winter, spring, summer and autumn, respectively, while the overall median average is 0.70 arcsec. This value is higher than the median seeing in the first two campaigns and lower than the results in this paper (see Section 4.6). The differences show the skewness produced by uneven coverage during the year in all three campaigns.

Our global seeing results are in good agreement with those of Skidmore et al. (2009). The slight differences found could be the result of a larger temporal coverage in our data set, from 2004 October to 2008 August.

If we compare the results in this work (Table 8) with those of previous studies (see Table 1 and Section 4.3), we find that the whole atmosphere seeing (ε_{DIMM}) is larger than most of the values

reported previously. This could be the result of a slight degradation in seeing in recent years.

Based on the results for Paranal and La Silla (Sarazin et al. 2008), we suggest that the apparent seeing degradation found at SPM might be correlated with climate change.[1] We have consulted the Climatic Data Base of North-West Mexico (http://peac-bc.cicese.mx/datosclim), which contains weather data for a number of stations near the SPM observatory site for the years 1981–2008. For this time period, we found that the temperature tends to increase by 0.05 °C per year, while the water precipitation tends to decrease by 5 mm per year. These variations clearly point to a climate change that might produce local effects. Whether the seeing degradation is a result of these effects has yet to be established. However, a full study of the dependence of the seeing value with the SPM climate change is beyond the scope of this paper.

From a statistical point of view, we have found that the seeing at SPM does not suffer any degradation towards dawn, in contrast with the results reported by Skidmore et al. (2009). However, the consistent increase of seeing values towards the end of the night might suggest, as Skidmore et al. (2009) have stated, that seeing degrades towards dawn. It would be necessary to collect a large number of observations towards dawn, so that this result could be established with a sufficient degree of statistical significance.

Carrasco et al. (2012) have studied SPM solar radiation (cloud coverage) using the TMT data for the same period presented in this paper. They have stated that SPM skies are clear in spring, relatively cloudy in summer and fairly clear in winter. It is interesting to notice that there appears to be a correlation between the cloud cover during day time and the nightly value of the seeing, in the sense that cloudy days have better seeing at night, and vice versa. This might indicate that the processes that occur when the cloud cover is dissipated contribute to smaller amounts of atmospheric turbulence. This is an interesting point that merits further study, which is beyond the scope of this work.

5 SUMMARY AND CONCLUSIONS

In this paper, we have used the data obtained by the TMT Site-Testing Project for the SPM site in the north-west of Mexico. The data consist of DIMM and MASS measurements taken over a period of nearly five years (2004 October to 2008 August, ∼1400 nights). A variety of previous studies have measured the seeing at SPM. The obtained median seeing varies from 0.50 to 0.79 arcsec, although these measurements have been taken in different epochs and with disparate instruments. The coverage of each observing run is also limited.

For the analysis presented in this paper, we have made a detailed coverage study, obtaining percentages of total observed time per night with respect to total night length. This is the first time that this approach has been presented in the seeing astronomical literature. The total coverages for DIMM, MASS and simultaneous data are 40.2, 27.9 and 26.4 per cent, respectively. This means that, of the 1400 available nights, the DIMM data were obtained in an equivalent of 563 'fully observed' nights (nights with a 100 per cent time coverage), whereas for the MASS this corresponds to 391 nights and for the simultaneous data it corresponds to 370 nights.

We have calculated nightly, monthly, seasonal, annual and global statistics of the seeing from MASS, DIMM and simultaneous MASS–DIMM observations. The simultaneous MASS–DIMM

---

[1] Sarazin M., 2010: http://www.eso.org/gen-fac/pubs/astclim/paranal/seeing/singstory.html.

results indicate that the best seeing is obtained for 2006 September (DIMM, 0.62 arcsec; MASS, 0.31 arcsec) and 2007 August (DIMM, 0.61 arcsec; MASS, 0.27 arcsec) . These months correspond to our definition of the summer season, in which the calculated seeing is 0.64, 0.33 and 0.46 arcsec, which are median values for DIMM, MASS and GL, respectively. This makes summer the best seeing season at SPM. It is worth noting that the seeing obtained for 2006 (DIMM, 0.74 arcsec; MASS, 0.37 arcsec; GL, 0.54 arcsec) is the best yearly seeing of the whole campaign, and it also corresponds to the best sampled year. For the GL seeing, the best month is July with a value of 0.45 arcsec. The overall results yield a median seeing of 0.78 arcsec (DIMM), 0.37 arcsec (MASS) and 0.59 arcsec (GL). Compared with previous works, we have found that our whole atmosphere seeing values are slightly larger than most of the values reported previously. Perhaps this is because of a degradation of seeing with time, which might be caused by climate effects. The hourly analysis clearly shows that there is no statistically significant tendency of seeing degradation towards dawn, in contrast with that reported by Skidmore (2009).

These results show that SPM is a competitive astronomical site, where it would be worth performing a continuous astroclimate evaluation.

ACKNOWLEDGMENTS

REFERENCES

Alvarez M., López E., 1982, in Corral M. A. M., ed., Simposio de Historia de la Astronomía en México. UNAM, Mexico, p. 311
Alvarez M., Maisterrena Y., 1977, Rev. Mex. Astron. Astrofis., 2, 43
Alvarez M., Michel R., Reyes-Coca S., Troncoso-Gaytán R., 2007, Rev. Mex. Astron. Astrofis. Ser. Conf., 31, 13
Araiza Quijano M. R., Cruz-González I., 2011, Rev. Mex. Astron. Astrofis., 47, 409
Avila R., Cuevas S., 2009, Optics Express, 17, 10926
Avila R., Vernin J., Cuevas S., 1998, PASP, 110, 1106
Avila R., Masciadri E., Vernin J., Sánchez L. J., 2004, PASP, 116, 682
Avila R., Carrasco E., Ibañez F., Vernin J., Prieur J.-L., Cruz D. X., 2006, PASP, 118, 503
Avila R., Sánchez L. J., Ibañez F., Vernin J., Masciadri E., Azouit M., Agabi A., Cuevas S., 2007, Rev. Mex. Astron. Astrofis. Ser. Conf., 31, 71
Avila R., Sánchez L. J., Cruz-González I., Castaño V. M., Carrasco E., 2011, Rev. Mex. Astron. Astrofis., 47, 75
Bohigas J., Núñez J. M., 2010, Rev. Mex. Astron. Astrofis., 46, 89
Bohigas J. et al., 2008, Rev. Mex. Astron. Astrofis., 44, 231
Carrasco E., Sarazin M., 2003, Rev. Mex. Astron. Astrofis. Ser. Conf., 19, 103
Carrasco E., Avila R., Carramiñana A., 2005, PASP, 117, 104
Carrasco E., Carramiñana A., Sánchez L. J., Avila R., Cruz-González I., 2012, MNRAS, 420, 1273
Conan R. et al., 2002, A&A, 396, 723
Cruz-González I., Avila R., Tapia M., eds., 2003, Rev. Mex. Astron. Astrofis. Ser. Conf., 19
Cruz-González I. et al., 2004, Proc. SPIE, 5382, 634
Echevarría J., 2003, Rev. Mex. Astron. Astrofis. Ser. Conf., 19, 41
Echevarría J. et al., 1998, Rev. Mex. Astron. Astrofis., 34, 47
Els S. G. et al., 2008, Appl. Opt., 47, 2610
Els S. G., Travouillon T., Schöck M., Riddle R., Skidmore W., Seguel J., Bustos E., Walker D., 2009, PASP, 121, 527
Fried D. L., Mevers G. E., 1974, Appl. Opt., 13, 2620
Hiriart D., 2003, Rev. Mex. Astron. Astrofis. Ser. Conf., 19, 90
Hiriart D., Ochoa J. L., García B., 2001, Rev. Mex. Astron. Astrofis., 37, 213
Kornilov V., Tokovinin A., Shatsky N., Voziakova O., Potanin S., Safonov B., 2007, MNRAS, 382, 1268
Masciadri E., Garfias T., 2001, A&A, 366, 708
Masciadri E., Avila R., Sánchez L. J., 2002, A&A, 382, 378
Masciadri E., Avila R., Sánchez L. J., Cuevas S., Garfias F., Agabi A., Azouit M., Vernin J., 2003, Rev. Mex. Astron. Astrofis. Ser. Conf., 19, 63
Masciadri E., Avila R., Sánchez L. J., 2004, Rev. Mex. Astron. Astrofis., 40, 3
Mendoza E. E., 1971, Bol. Obs. Tonantzintla Tacubaya, 6, 95
Mendoza E. E., 1973, Mercury, 2, 9
Mendoza E. E., Luna J., Gómez T., 1972, Bol. Obs. Tonantzintla Tacubaya, 6, 215
Michel R., Echevarría J., Costero R., Harris O., 2003a, Rev. Mex. Astron. Astrofis. Ser. Conf., 19, 37
Michel R., Echevarría J., Costero R., Harris O., Magallón J., Escalante K., 2003b, Rev. Mex. Astron. Astrofis., 39, 291
Michel R., Hiriart D., Chapela A., 2003c, Rev. Mex. Astron. Astrofis. Ser. Conf., 19, 99
Otárola A., Hiriart D., Pérez-León J. E., 2009, Rev. Mex. Astron. Astrofis., 45, 161
Parrao L., Schuster W. J., 2003, Rev. Mex. Astron. Astrofis. Ser. Conf., 19, 81
Riddle R. L., Schöck M., Skidmore W., 2006, Proc. SPIE, 6267, 56
Roddier F., 1981, Progress in Optics, Vol. 19. North-Holland, Amsterdam, p. 281
Sánchez L. J. et al., 2003, Rev. Mex. Astron. Astrofis. Ser. Conf., 19, 23
Sánchez L. J. et al., 2007, Rev. Mex. Astron. Astrofis. Ser. Conf., 31, 93
Sarazin M., Roddier F., 1990, A&A, 227, 294
Sarazin M., Melnick J., Navarrete J., Lombardi G., 2008, The Messenger, 132, 11
Schöck M. et al., 2009, PASP, 121, 384
Schöck M., Els S., Otárola A., Riddle R., Skidmore W., Travouillon T., Proc. SPIE, 7736, 66
Schuster W. J., Parrao L., 2001, Rev. Mex. Astron. Astrofis., 37, 187
Skidmore W., Els S., Travouillon T., Riddle R., Schöck M., Bustos E., Seguel J., Walker D., 2009, PASP, 121, 1151
Sohn E., 2007, Rev. Mex. Astron. Astrofis. Ser. Conf., 31, 122
Tapia M., 1992, Rev. Mex. Astron. Astrofis., 24, 179
Tapia M., 2003, Rev. Mex. Astron. Astrofis. Ser. Conf., 19, 75
Tapia M., Cruz-González I., Avila R., 2007a, Rev. Mex. Astron. Astrofis. Ser. Conf., 28, 9
Tapia M., Cruz-González I., Hiriart D., Richer M., 2007b, Rev. Mex. Astron. Astrofis. Ser. Conf., 31, 47
Tokovinin A., 2007, Rev. Mex. Astron. Astrofis. Ser. Conf., 31, 61
Tokovinin A., Kornilov V., 2007, MNRAS, 381, 1179
Tokovinin A., Kornilov V., Shatsky N., Voziakova O., 2003, MNRAS, 343, 891
Tokovinin A., Vernin J., Ziad A., Chun M., 2005, PASP, 117, 395
Vogiatzis K., Hiriart D., 2004, Rev. Mex. Astron. Astrofis., 40, 81
Walker M. F., 1971, PASP, 83, 401
Walker M. F., 1984, in Ardeberg A., Woltjer L., eds, Proc. ESO Workshop on Site Testing for Future Large Telescopes, Vol. 18. ESO, Garching, p. 3
Wang L. et al., 2007, Appl. Opt., 46, 6460
Wehinger P., 2007, Rev. Mex. Astron. Astrofis. Ser. Conf., 28, 1

This paper has been typeset from a TEX/LATEX file prepared by the author.